

一价金的氮氧自由基配合物的合成、结构及其磁性

李承辉 顾志国 左景林* 游效曾

(南京大学配位化学研究所, 配位化学国家重点实验室, 南京 210093)

摘要: 本文合成了一个含一价金的氮氧自由基配合物 $(\text{PPh}_3)\text{Au}(p\text{-NN})$ (**1**) [$p\text{-NN}=2\text{-(对-乙炔基苯基)-4,4,5,5-四甲基-2-咪唑啉基氧自由基}$], 并用 X 射线衍射单晶结构分析测定了它的结构。由于三苯基膦具有较大的位阻效应, 因此配合物中不存在明显的分子内或分子间 $\text{Au}\cdots\text{Au}$ 相互作用。磁化率研究表明, 相邻分子间的 $\text{O}\cdots\text{O}$ 相互作用使之形成二聚体, 因而导致了分子之间的反铁磁相互作用。

关键词: 一价金配合物; 氮氧自由基; 磁性

中图分类号: O614.123

文献标识码: A

文章编号: 1001-4861(2007)09-1582-05

Synthesis, Structure and Magnetic Property of a Gold(I) Complex with Nitronyl-nitroxide Radical

LI Cheng-Hui GU Zhi-Guo ZUO Jing-Lin* YOU Xiao-Zeng

(Coordination Chemistry Institute and the State Key Laboratory of Coordination Chemistry, Nanjing University, Nanjing 210093)

Abstract: The complex $(\text{PPh}_3)\text{Au}(p\text{-NN})$ (**1**), where $p\text{-NN}=2\text{-(p-Ethynylphenyl)-4,4,5,5-tetramethyl-2-imidazoline-1-oxide-3-oxyl}$ has been prepared and structurally characterized. No close intra- or inter-molecular $\text{Au}\cdots\text{Au}$ contact was found in the structure of complex **1** due to the steric hindrance of the bulky triphenylphosphine ligand. Magnetic studies show inter-molecular anti-ferromagnetic interactions which result from the dimerized structure formed by short $\text{O}\cdots\text{O}$ contact between neighboring molecules. CCDC: 646346.

Key words: gold(I) complex; nitronyl-nitroxide radical; magnetic property

0 Introduction

In the preparation of molecule based magnetic materials, transition metal complexes with organic radical ligands have been found widespread interest in recent years^[1,2]. Most of the work in this topic has been focused on the well known Ulman's nitronyl-nitroxide family of radicals since they are stable and easy to functionalize^[3]. A wide variety of transition metal complexes have been prepared with these ligands, most of them involving paramagnetic transition metal

coordinated to the NO group. Strong metal-ligand magnetic exchange interactions have been observed from the radicals to paramagnetic transition-metal ions. On the other hand, incorporation of diamagnetic-metal into these "metal-radical" systems represents another strategy to construct molecular magnetic material where the metal ions play an active role in aiding the exchange coupling between the radicals. Several diamagnetic-metal complexes with organic radical ligands exhibiting operative antiferro- or ferro-magnetic interactions have been reported, such as those of Ti(IV) ,

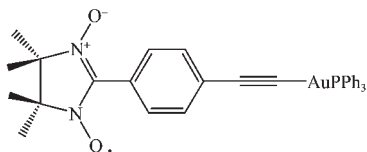
收稿日期: 2007-06-12。收修稿日期: 2007-08-17。

国家自然科学基金项目(No.20531040)、国家重点基础研究发展计划项目(No.2006CB806104)资助。

*通讯联系人。E-mail: zuojl@nju.edu.cn

第一作者: 李承辉, 男, 28岁, 博士研究生; 研究方向: 功能配合物。

Cu(I), Ag(I), Hg(II), Zn(II), and Cd(II)^[4-10]. However, there are very few examples of gold (I) ions being incorporated into molecular magnetic materials^[11]. Herein, we report the synthesis, structure characterization and magnetic property of a new gold(I) complex containing nitronyl-nitroxide radical (Scheme 1).



Scheme 1

1 Experimental

1.1 Reagent and apparatus

All reactions were carried out under a nitrogen atmosphere using standard Schlenk and vacuum line technique. Chemicals were obtained from commercial resources and used without further purification. The solvents were treated using the common method for preparing anhydrous and deoxygenated solvents. Column separation was carried out using 160~200 mesh silica gel. $(\text{PPh}_3)\text{AuCl}$ ^[12] and the para-ethynyl-phenylnitronyl-nitroxide radical^[13] were prepared according to the literature.

The IR spectrum was taken on a Vector22 Bruker Spectrophotometer ($400\sim 4\,000\text{ cm}^{-1}$) with KBr pellets. The UV-Vis spectrum was recorded on a Shimadzu UV-3100 spectrometer. The magnetic susceptibility was measured using a Quantum Design MPMS-XL7 SQUID magnetometer at temperature ranging from 1.8 to 300 K and using an applied magnetic field of 2 000 Oe. ESR spectrum was measured using a Bruker ER 200-D-SRC spectrometer. Elemental analysis for C, H, and N were performed on a Perkin-Elmer 240C analyzer.

1.2 Synthesis of $(\text{PPh}_3)\text{Au}(p\text{-NN})$ (**1**)

Under nitrogen atmosphere, a methanol solution (30 mL) containing NaOH (0.028 5 g, 0.7 mmol) and ethynyl-(4,4,5,5-tetramethyl-4,5-dihydro-1H-imidazol-1-yloxy)-phenyl (0.184 g, 0.7 mmol) was added into 30 mL of dichloromethane with $(\text{PPh}_3)\text{AuCl}$ (0.352 g, 0.7 mmol). The reaction mixture was stirred at room temperature for 5 h. The solvent was evaporated and the residue was separated on $2.5 \times 30\text{ cm}$ silica gel chromatography using CH_2Cl_2 as eluent. Yield 0.186 g (37%). Anal. Calcd. for $\text{C}_{33}\text{H}_{31}\text{AuN}_2\text{O}_2\text{P}$ (%): C, 55.39; H, 4.37; N, 3.91. Found: C, 55.20; H, 4.51; N, 4.05. IR (KBr, cm^{-1}): 2 115 ($\nu_{\text{C}=\text{C}}$), 1 358 (ν_{NO}). UV-Vis (CH_2Cl_2) λ , nm (ϵ , $\text{mol}^{-1} \cdot \text{cm}^{-1}$): 311 (49 150), 329 (48 040), 348(13 240), 602(502).

1.3 Crystal structure determination

The well-shaped single crystal of **1** was selected for X-ray diffraction study on a Siemens (Bruker) SMART CCD diffractometer using graphite monochromated Mo $K\alpha$ radiation ($\lambda=0.071\,073\text{ nm}$). Cell parameters were retrieved using SMART software and refined using SAINT on all observed reflections^[14]. Data were collected using a narrow-frame method with scan widths of 0.30° in ω and an exposure time of 5 s per frame. The highly redundant data sets were reduced using SAINT and corrected for Lorentz and polarization effects. Absorption corrections were applied using SADABS supplied by Bruker^[15]. The structure was solved by direct methods and refined on F^2 by full-matrix least-squares procedures using SHELXTL software^[16]. All non-hydrogen atoms were anisotropically refined. The hydrogen atoms were located theoretically and not refined. Crystallographic data and refinement for the complex are presented in Table 1.

Table 1 Crystal data and structure refinement for complex 1

Formula	$\text{C}_{33}\text{H}_{31}\text{AuN}_2\text{O}_2\text{P}$	Absorption coefficient / mm	5.105
Formula weight	715.53	$F(000)$	1 412
Temperature / K	293(2)	θ range / ($^\circ$)	2.00~25.02
Crystal system	Monoclinic	Limiting indices (h, k, l)	$-16 \leq h \leq 16, -9 \leq k \leq 15, -20 \leq l \leq 20$
Space group	$P2_1/c$	Reflections collected	14 431
a / nm	1.386 0(16)	Independent reflection (R_{int})	5 180 (0.030 5)
b / nm	1.323 2(15)	Reflections [$I > 2\sigma(I)$]	4 227
c / nm	1.696 5(19)	Data / restraints / parameters	5 180 / 0 / 356

Continued Table 1

$\beta / (^{\circ})$	109.60(2)	Goodness-of-fit on F^2	1.071
Z	4	Final R indices [$I > 2\sigma(I)$]	$R_1=0.038\ 1$, $wR_2=0.084\ 5$
V / nm^3	2.931\ 2(6)	Largest diff. peak and hole / ($\text{e} \cdot \text{nm}^{-3}$)	45 and -138
$D_{\text{calc}} / (\text{g} \cdot \text{cm}^{-3})$	1.621		

CCDC: 646346.

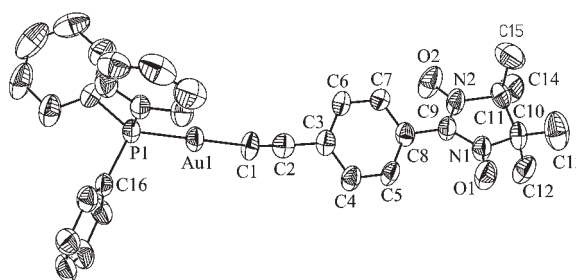
2 Results and discussion

2.1 Crystal structure

Complex **1** crystallizes in space group $P2_1/c$. The molecular structure is shown in Fig.1. Selected bond distances and angles are listed in Table 2. A linearly coordinated gold(I) center with the P-Au-C angle of $177.4(3)^{\circ}$ is observed and the bond lengths of Au-P and Au-C are 0.227 1(2) nm and 0.199 8(9) nm, respectively. The N-O bond length of 0.127 1(9)~0.127 5(8) nm is comparable with those of other systems containing this fragment. The dihedral angle between the planes of nitronyl-nitroxide fragment and phenyl group is 38.17° . The neighboring molecules are arranged in the head-to-head fashion through shorter $\text{O} \cdots \text{O}$ contact [$\text{O}(1) \cdots \text{O}(1')$ 0.337 8 nm], leading to a dimerized structure (Fig.2).

It is noteworthy that no close intermolecular $\text{Au} \cdots \text{Au}$ interaction was found in the structure of complex **1**, in spite of that aurophilic interactions are frequently observed in gold(I) complexes. This may be

due to the bulky ligand of triphenylphosphine which inhibits the close contact of two gold(I) centers.



Thermal ellipsoids are drawn at the 50% probability levels
H atoms are omitted for clarity

Fig.1 Perspective drawing of complex **1** showing the atom numbering

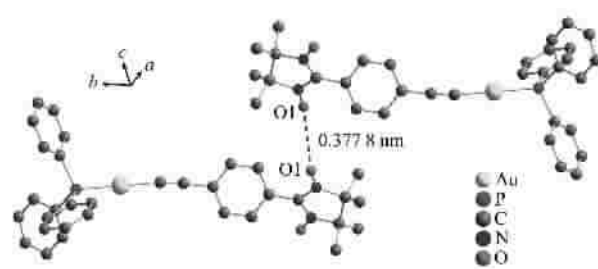


Fig.2 View of the "dimmer" structure formed through short $\text{O} \cdots \text{O}$ contact

Table 2 Selected bond distances (nm) and bond angles ($^{\circ}$) for complex **1**

Au(1)-P(1)	0.227 1(13)	Au(1)-C(1)	0.200 4(5)	C(1)-C(2)	0.115 3(7)
C(2)-C(3)	0.147 3(7)	C(9)-N(1)	0.132 3(7)	C(9)-N(2)	0.135 4(7)
C(10)-N(1)	0.151 9(7)	C(11)-N(2)	0.150 4(7)	N(1)-O(1)	0.127 6(6)
N(2)-O(2)	0.127 8(6)				
P(1)-Au(1)-C(1)	177.17(15)	C(8)-C(9)-N(1)	125.80(5)	C(9)-N(1)-C(10)	111.90(4)
Au(1)-C(1)-C(2)	171.80(6)	N(1)-C(9)-N(2)	110.60(5)	C(9)-N(2)-O(2)	126.70(5)
C(1)-C(2)-C(3)	175.60(6)	C(9)-N(1)-O(1)	127.30(5)	O(2)-N(2)-C(11)	123.00(5)
C(8)-C(9)-N(2)	123.60(5)	O(1)-N(1)-C(10)	120.80(5)	C(9)-N(2)-C(11)	110.20(5)

2.2 ESR spectrum

The ESR spectrum of complex **1** consists of five main lines due to the hyperfine coupling (hfc) of electron spin with two equivalent nitronyl-nitroxide nitrogen atoms (^{14}N) (Fig.3). These lines centered at $g=2.006\ 3$ has an intensity ratio of 1:2:3:2:1 which is

characteristic of monoradical complex ^[17]. Possible hyperfine splitting with the hydrogen atoms in the phenyl ring was not observed in this case.

2.3 Magnetic properties

The variable temperature magnetic susceptibility data for a polycrystalline sample of complex **1** was

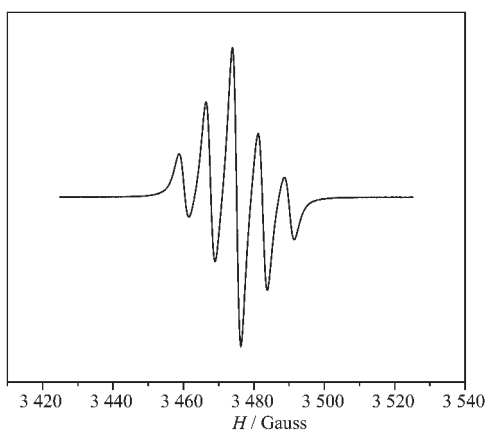
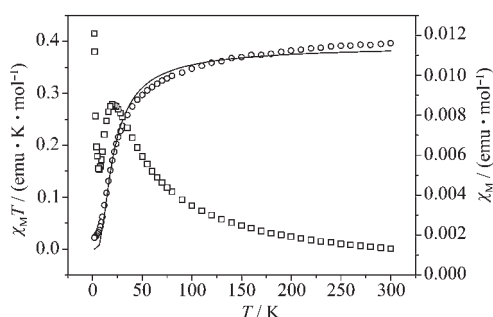


Fig.3 ESR spectrum of complex **1** in CH_2Cl_2 solution ($5 \times 10^{-4} \text{ mol} \cdot \text{L}^{-1}$) at 298 K

measured on SQUID susceptometer over the temperature range 1.8~300 K with an applied field of 2 000 Oe. The plots of $\chi_{\text{M}}T$ and χ_{M} vs T are shown in Fig.4. The $\chi_{\text{M}}T$ value of $0.39 \text{ emu} \cdot \text{K} \cdot \text{mol}^{-1}$ was observed at room temperature, which is slightly higher than the value required for uncorrelated spin 1/2 ($\chi_{\text{M}}T=0.375 \text{ emu} \cdot \text{K} \cdot \text{mol}^{-1}$) in mono-radical complex. Upon cooling, the $\chi_{\text{M}}T$ value decreases gradually from 300 to 75 K, and then decreases sharply with the temperature further lowered. The χ_{M} vs T curve is increasing with the temperature, reaching to a plateau between 10 and 30 K ($\chi_{\text{M}}=0.0085 \text{ emu} \cdot \text{mol}^{-1}$). At very low temperature, a Curie tail is observed due to some paramagnetic impurity. This magnetic behavior indicated the presence of anti-ferromagnetic interactions in the complex.



Solid line corresponds to the best theoretical fit

Fig.4 Plot of $\chi_{\text{M}}T$ (○) and χ_{M} (□) vs T for complex **1**

As described above, complex **1** shows a dimerized structure through shorter O...O contact. Therefore, the magnetic data could be fitted by Bleaney and Bowers equation (eq 1) for dimeric

system:

$$\chi = \frac{2Ng^2\beta^2}{kT} \frac{1}{3 + e^{-\frac{2J}{kT}}} \quad (1)$$

The least-square analysis of the magnetic susceptibility data led to $J=-12.8(1) \text{ cm}^{-1}$, $g=2.049(3)$, and $R=1.9 \times 10^{-4}$ (the agreement factor defined as $R = \sum [(\chi_{\text{obsd}} - \chi_{\text{calcd}})^2 / \chi_{\text{obsd}}^2]$).

3 Conclusion

In this paper, a new gold(I) phosphine complex containing the ethynyl-phenyl-nitronyl-nitroxide radical has been prepared. No aurophilic interaction was found in the crystal structure of complex **1**. The magnetic studies show inter-molecular anti-ferromagnetic interactions which result from the dimerized structure formed by shorter O...O contact between neighboring molecules.

References:

- [1] Lemaire M T. *Pure Appl. Chem.*, **2004**, **76**:277~293
- [2] Caneschi A, Caneschi D, Sessoli R, et al. *Acc. Chem. Res.*, **1989**, **22**:392~398
- [3] Osiecki J H, Ullman E F. *J. Am. Chem. Soc.*, **1968**, **90**:1078~1079
- [4] Caneschi A, Dei A, Gatteschi D. *J. Chem. Soc. Chem. Commun.*, **1992**:630~631
- [5] Bruni S, Aneschi A, Cariati F, et al. *J. Am. Chem. Soc.*, **1994**, **116**:1388~1394
- [6] (a) Oshio H, Watanabe T, Ohto A, et al. *Angew. Chem. Int. Ed.*, **1994**, **33**:670~671
(b) Oshio H, Watanabe T, Ohto A, et al. *Inorg. Chem.*, **1996**, **35**:472~475
(c) Oshio H, Watanabe T, Ohto A, et al. *Inorg. Chem.*, **1997**, **36**:3014~3021
(d) Oshio H, Yamamoto M, Hoshino N, et al. *Polyhedron*, **2001**, **20**:1621~1625
(e) Oshio H, Yamamoto M, Ito T, et al. *Inorg. Chem.*, **2001**, **40**:5518~5525
- [7] (a) Lee C J, Huang C H, Wei H H, et al. *J. Chem. Soc. Dalton. Trans.*, **1998**:171~176
(b) Lee C J, Wei H H. *Inorg. Chem. Acta*, **2000**, **310**:89~95
(c) Lee C J, Wei H H, Lee G H, et al. *Inorg. Chem. Commun.*, **2000**, **3**:690~693
- [8] Storh C, Belorizky E, Turek P, et al. *Inorg. Chem.*, **2003**, **42**:2938~2949
- [9] Francesse G, Romero F M, Neels A, et al. *Inorg. Chem.*,

- 2000,39**:2087~2095
- [10](a)Wang S P, Li D J, Song Y, et al. *Z. Anorg. Allg. Chem.*, **2005,631**:1702~1705
- (b)Wang S P, Gao D Z, Liao D Z, et al. *Trans. Met. Chem.*, **2006,31**:214~219
- [11]Leznoff D B, Rancurel C, Sutter J P, et al. *J. Chem. Soc., Dalton. Trans.*, **1999**:3593~3599
- [12]Al-sa'ady A K, Mcauliffe C A, Parish R V, et al. *Inorg. Synth.*, **1985,23**:191~194
- [13]Wautelet P, Moigne J L, Videva V, et al. *J. Org. Chem.*, **2003**, **68**:8025~8036
- [14]Siemens, *SAINT, v4 Software Reference Manual*, Siemens Analytical X-ray Systems, Inc., Madison, WI, USA, **1996**.
- [15]Sheldrick G M. *SADABS, Program for Empirical Absorption Correction of Area Detector Data*, University of Göttingen, Göttingen, Germany, **1996**.
- [16]Siemens, *SHELXTL, Version 5.1 Reference Manual*, Siemens Analytical X-ray Systems, Inc., Madison, WI, USA, **1996**.
- [17]Fujii A, Ishida T, Koga N, et al. *Macromolecules*, **1991,24**: 1077~1082